High-spin states and signature inversion in ^{78}Br

E. Landulfo,[1,2,4] D. F. Winchell,[1] J. X. Saladin,[1] F. Cristancho,[1,*] D. E. Archer,[3] J. Döring,[3] G. D. Johns,[3] M. A. Riley,[3] S. L. Tabor,[3] V. A. Wood,[3] S. Salém-Vasconcelos,[2] and O. Dietzsch[2]

[1]*Department of Physics, University of Pittsburgh, Pittsburgh, Pennsylvania 15260*

[2]*Instituto de Física, Universidade de São Paulo, 05508 São Paulo, Brazil*

[3]*Department of Physics, Florida State University, Tallahassee, Florida 32306*

[4]*Instituto de Pesquisas Energéticas e Nucleares-IPEN/CNEN SP, CP 11049-CEP 05422-970 São Paulo, Brazil*

(Received 21 March 1996)

High-spin states in ^{78}Br have been studied up to an excitation energy of approximately 6 MeV and a spin of $17\hbar$ using the ^{70}Zn(^{11}B,3n)^{78}Br reaction at a beam energy of 45 MeV. The properties of the observed rotational bands, including moments of inertia, signature splitting, and signature inversion, are discussed within the context of the cranked shell model. It is shown that cranked-shell-model calculations are able to reproduce the experimentally observed signature inversion in the positive-parity yrast bands in the odd-odd isotopes ^{74,76,78}Br, which permits the assignments of quasiparticle configurations to these bands. [S0556-2813(96)01808-0]

PACS number(s): 21.10.Re, 21.60.Jz, 23.20.Lv, 27.50.+e

I. INTRODUCTION

The spectroscopy of high angular momentum states in nuclei in the mass $A\approx 80$ region is a topic of considerable interest. Phenomena found in this region include large deformation, shape coexistence, and, quite often, rapid variation of structure with changes in neutron and/or proton number. In addition, protons and neutrons in this mass region occupy the same subshells, enhancing the possibility of studying residual proton-neutron interactions. The investigation of odd-odd bromine ($Z=35$) isotopes, as well their isobaric neighbors, has been useful in furthering our understanding of the interplay of one and two quasiparticle states with collective excitations.

The variety of shapes in this region has been studied extensively both experimentally and theoretically. For ^{74}Br, calculations show a minimum in the energy surface for a deformation of $(\beta_2,\gamma) = (0.33,-4°)$ [1]. A more triaxial shape, with $(\beta_2,\gamma) \approx (0.35,20°)$, has been suggested for ^{76}Br [2]. Lifetime measurements have confirmed a quadrupole deformation of $\beta_2\approx 0.30$ in this nucleus [3]. Cranked-shell-model calculations predict a triaxial deformation of $\gamma\approx 30°$ for the lowest positive-parity configuration in ^{77}Br [4]. Triaxial deformations are also predicted for ^{79}Kr [5] and ^{82}Y [6], which are isotones of ^{78}Br. Lifetime measurements in ^{82}Y indicate a transition from near-spherical shape at low spin to a well-deformed quadrupole deformation at high spin [7].

An interesting feature found in the light odd-odd bromine isotopes ^{74,76}Br is a signature inversion in the positive-parity yrast band. This band is built on an isomeric 4^+ state and is based on a $\pi g_{9/2}\otimes \nu g_{9/2}$ configuration. ''Signature inversion'' describes the phenomenon in which the signature that is energetically favored at low spin ($\alpha=0$ in this case) becomes unfavored at higher spin. In addition to ^{74}Br [8] and ^{76}Br [3,9], signature inversion is also observed in the positive-parity yrast bands in ^{80}Rb [10], ^{82}Y [6], and ^{84}Nb [11].

Both cranked mean-field and particle-rotor models have been used in trying to understand the origins of signature inversion. Bengtsson *et al.* [12] suggest that, for certain particle numbers, a signature-inverted spectrum can be obtained in the cranked mean-field approach when a triaxially deformed nucleus is cranked around the shortest axis ($\gamma>0°$ in the Lund convention). According to this model, signature inversion can occur in the $A\approx 80$ mass region in nuclei with proton or neutron numbers between 39 and 47. In the particle-rotor approach, triaxiality may or may not be needed to explain signature inversion, depending on the specific case. In a study of ^{76}Br, Kreiner and Mariscotti [13] predicted the previously unobserved signature inversion in the yrast band using a two-quasiparticle-plus-rotor model with an axially symmetric core. On the other hand, two-quasiparticle-plus-rotor calculations for ^{82}Y [6] indicate that signature inversion occurs only when a triaxial shape is assumed, though the results are only in qualitative agreement with experiment. Similar calculations in the rare-earth region [14] showed that signature inversion could be reproduced for an axially symmetric shape if a residual proton-neutron interaction was included in the Hamiltonian.

Before the present work, the highest spin known in ^{78}Br was $I^\pi=11^+$ at an energy of 1941 keV [15,16]. An additional tentative level at 2585 keV was reported in Ref. [15] but was not assigned a spin. At those energies, it is not clear whether or not signature inversion is occurring in the positive-parity yrast band. The work in Ref. [15] was done using an (α,pn) reaction. The work in Ref. [16] used $(\alpha,p2n)$ and (^{7}Li,5n) reactions, and report a somewhat different level scheme than that given in Ref. [15]. In Ref. [16] an interpretation of the nuclear structure of the low-lying states in terms of a two-quasiparticle-plus-rotor model calculation was performed, and it was found that, below the 9^+ state, the level scheme could be reproduced with very little

*Present address: Centro Internacional de Fisica, Bogota, Columbia.

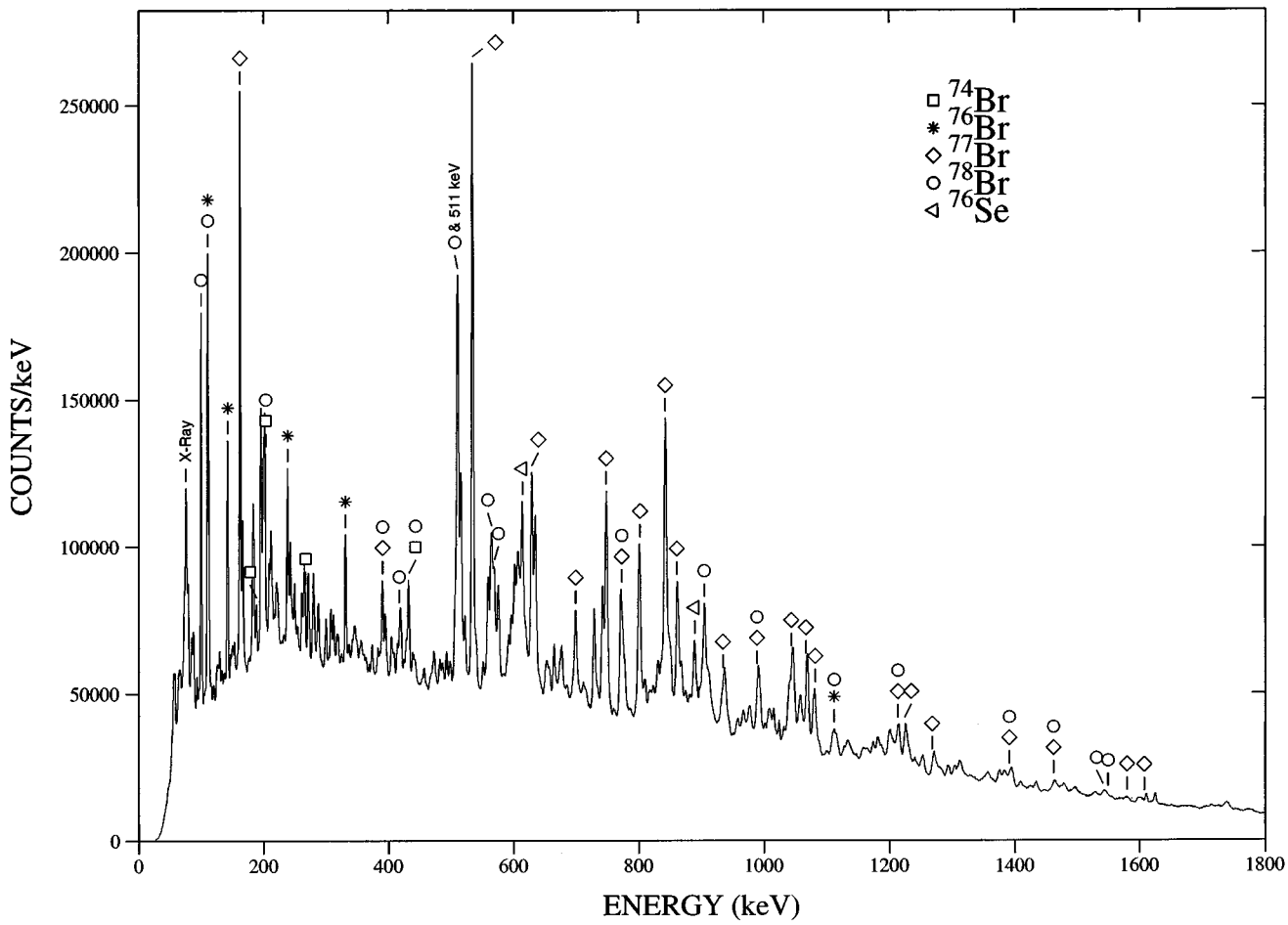

FIG. 1. A spectrum showing the total projection of the coincidence matrix. Origins of the strongest lines are indicated by symbols.

core rotation. This implies that the low-lying states are not collective excitations; they arise primarily from excitations of the unpaired particles. A deformation of $\beta=0.27$ was used in the calculation. Neither work reports finding negative-parity bands, though both positive- and negative-parity rotational bands have been found in ^{74}Br and ^{76}Br. The present experiment was designed to extend the level scheme of ^{78}Br in order to look for the expected signature inversion, as well as to look for additional rotational bands.

II. EXPERIMENTAL METHODS

High-spin states in ^{78}Br were populated using the reaction ^{70}Zn(^{11}B,3n). The Florida State University (FSU) Tandem-Linac facility was used to produce a 45 MeV ^{11}B beam. The target consisted of a stack of two 0.6 mg/cm^2 zinc foils enriched to 71% in ^{70}Zn. Typical beam current on target was 40 electrical nA. Besides the 3n channel, the strongest was the 4n channel, which formed ^{77}Br. Less intense were the pxn channels, which populated some Se isotopes. Because of ^{66}Zn and ^{68}Zn impurities in the target, ^{74}Br and ^{76}Br exit channels were also relatively well populated.

The Pitt-FSU detector array [17,18] was used for γ-ray detection. It consisted of nine high-purity germanium (HPGe) detectors with Compton suppression and a 28-element bismuth germanate sum-energy and multiplicity spectrometer (SMS). Four of the HPGe detectors were placed at 90° relative to beam line, four at 145°, and one at 35°. The event trigger required at least two HPGe detectors and at least one SMS element to fire. The latter requirement enhanced the selection of high angular momentum events. Data were collected in event-by-event mode and stored on magnetic tape. The energy and global efficiency calibrations of the detectors were determined by taking off-line spectra from ^{152}Eu and ^{133}Ba standard sources. Known in-beam lines in the spectra from ^{76}Br, ^{77}Br, and ^{78}Br provided information for Doppler-shift compensation. Approximately 5×10^7 coincidence events were recorded on tape for subsequent analysis. Events were gain shifted and corrected for Doppler effect and histogrammed in an E_γ-E_γ matrix with a dispersion of 0.6 keV/channel. A second matrix was also constructed by sorting events in which a 90° and either a 35° or 145° detector fired, which provided data to perform a directional correlation of oriented nuclei (DCO) analysis, in order to determine multipolarities and help in the assignment of spins.

III. RESULTS

A total projection of the coincidence matrix is shown in Fig. 1, with symbols indicating the exit channels associated with the strongest lines. Figure 2 shows a spectrum created by gating on the 100 keV transition ($7^+\rightarrow6^+$) in ^{78}Br. Transitions from several rotational sequences can be seen in this

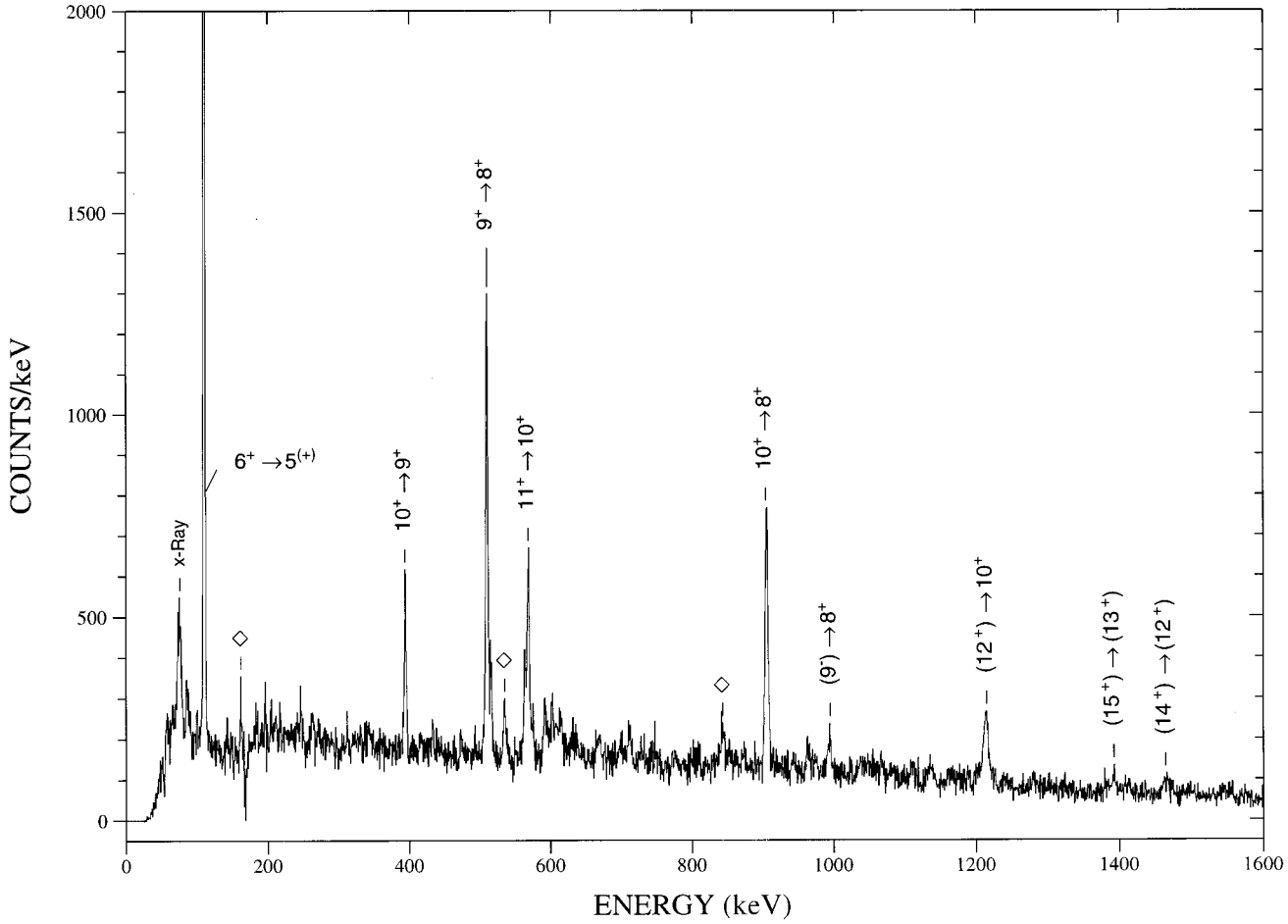

FIG. 2. The spectrum of γ rays created by gating on the 100 keV line. Diamonds indicate transitions in ^{77}Br.

spectrum. A partial level scheme of ^{78}Br showing the results of this and previous work [15,16] is given in Fig. 3. The low-energy detection threshold in the present experiment was about 50 keV; γ rays below that energy were not observed. Transitions in the low-spin, single-particle region observed in this work are in agreement with those seen in previous work [15]. New transitions and levels were placed based on coincidence relationships, systematics of neighboring nuclei, and, where possible, multipolarity assignments deduced from a DCO analysis. The DCO ratios (R_{DCO}) are defined as

$$R_{\mathrm{DCO}}=\frac{I(\gamma \text{ at } 35^\circ \text{ and/or } 145^\circ \text{ gated by } \gamma_G \text{ at } 90^\circ)}{I(\gamma \text{ at } 90^\circ \text{ gated by } \gamma_G \text{ at } 35^\circ \text{ and/or } 145^\circ)}, \quad (1)$$

where I is the intensity and the coincidence gate is always taken from an $E2$ transition. The DCO ratios for stretched electric quadrupole transitions are expected to have values close to unity, while $\Delta I=1$ transitions may have values ranging from 0 to 2, depending on the mixing ratio. For pure $M1$ transitions, R_{DCO} will have a value of 0.5. The results of the level determinations, with energies, intensities, multipolarities, spin assignments, and DCO ratios are shown in Table I. Altogether 16 new transitions were identified, corresponding to 11 new excited states in 4 rotational bands. The most energetic state observed has an energy of 6.088 MeV.

A. Positive-parity bands

Previously, the highest level observed in the positive-parity band was at 2585 keV, with no spin given. In the present experiment we extended this band to $I=17\hbar$, as shown in Fig. 3, which corresponds to seven new transitions belonging to this rotational band. A spectrum made by summing gates on the 394.8 and 904.6 keV, shown in Fig. 4, shows only transitions from the positive-parity band. The 32 keV $8^+\rightarrow 7^+$ and 47 keV $5^{(+)}\rightarrow 4^+$ transitions were not observed in this work, due to the low detection threshold. The DCO ratios for the $6^+\rightarrow 5^{(+)}$, $7^+\rightarrow 6^+$, and $11^+\rightarrow 10^+$ transitions all indicate the dipole nature of these transitions, while the ratios for the $(12^+)\rightarrow 10^+$ and $(13^+)\rightarrow 11^+$ transitions are consistent with that of a stretched $E2$ decay. The DCO ratio obtained for the $(13^+)\rightarrow(12^+)$ transition is consistent, within uncertanties, with either dipole or quadrupole multipolarity.

B. Negative-parity bands

A new band, feeding into the 227.7 keV $5^{(+)}$ level via a 196 keV transition, was also found. Transitions in the two

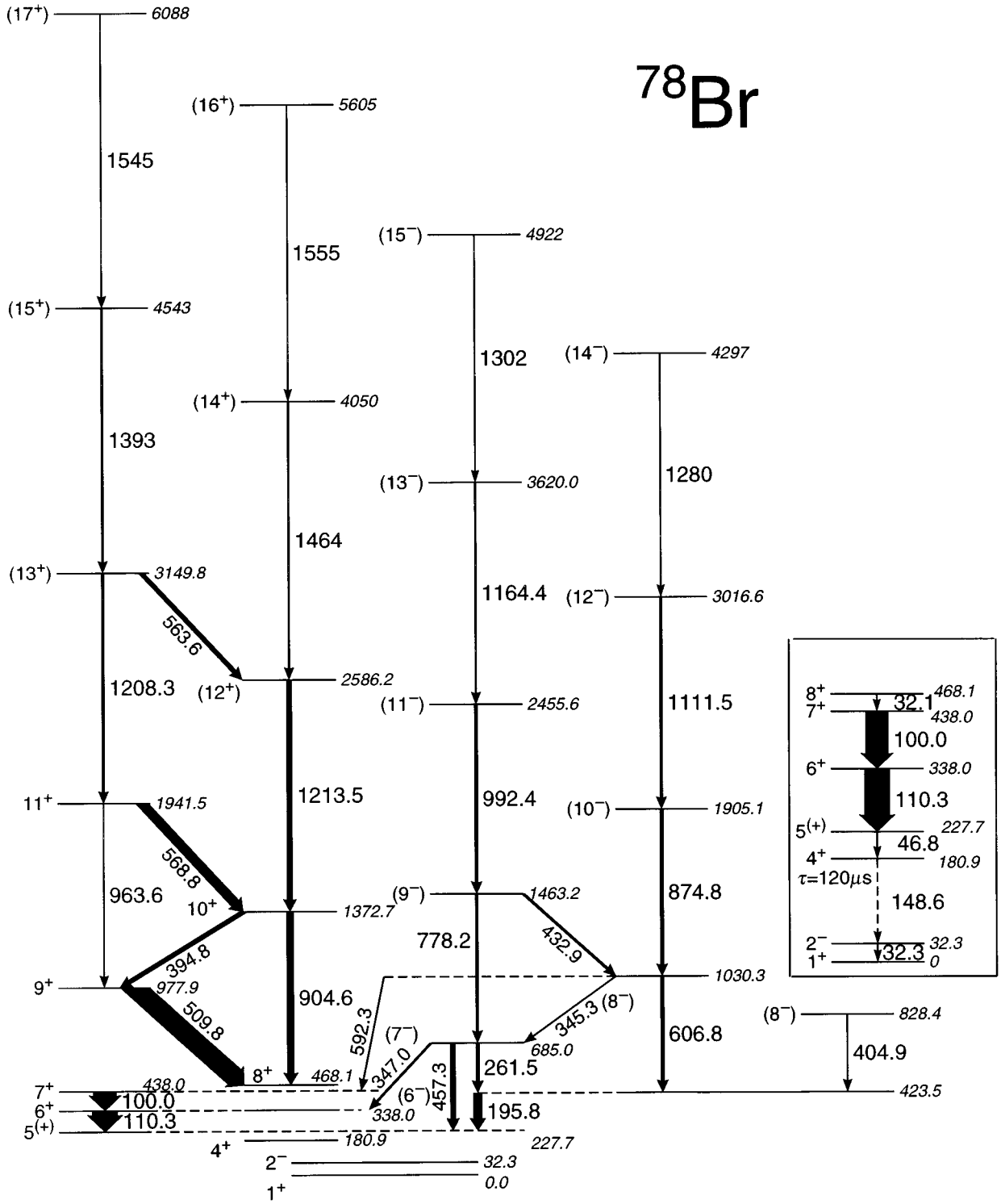

FIG. 3. Partial level scheme of ^{78}Br deduced from the present and previous works. The inset shows an expanded view of the lower part of the spectrum. The 148.8 keV transition from the 4^+ isomeric state was not observed in the present work, nor were the transitions with energy less than 50 keV.

signature partners of this band can be seen clearly in spectra created by gating on lines at 196 keV and 345 keV, as shown in Figs. 5 and 6. Previously, Döring *et al.* [15] observed the 196 keV line, as well as the 607 and 405 keV lines, but there were too few transitions to establish a band. The placement of the band in the level scheme is based on coincidence relationships. For instance, a gate on the 875 keV transition, feeding the level at 1030 keV, shows the 592, 606, 100, and 196 keV lines. Based on systematics, we have tentatively assigned negative parity to this band.

Previously, the position of the 196 keV transition in the level scheme was not well established. In Ref. [16], a 2^+ state at 196.0 keV is shown decaying directly to the ground state. Experiments using (p,n) reactions have reported states

TABLE I. Relative intensities and DCO ratios of γ rays observed in this work. Intensities are not corrected for internal conversion.

E_{level} (keV)	I_i^π	I_f^π	E_γ (kev)	Intensity [a]	R_{DCO}
338.0	6^+	$5^{(+)}$	110.3	123(9)	0.31(6)
423.5	(6^-)	$5^{(+)}$	195.8	36 (5)	
438.0	7^+	6^+	100.0	100(8)	0.51(9)
685.0	(7^-)	(6^-)	261.5	16(3)	
		6^+	347.0	11(2)	
		$5^{(+)}$	457.3	22(4)	
828.4	(8^-)	(6^-)	404.9	16(1)	
977.9	9^+	8^+	509.8	86(13)	
1030.3	(8^-)	(7^-)	345.3	7(1)	
		7^+	592.3	5(1)	
		(6^-)	606.8	38(3)	
1372.7	10^+	9^+	394.8	21(3)	
		8^+	904.6	110(16)	
1463.2	(9^-)	(8^-)	432.9	13(2)	
		(7^-)	778.2	29(5)	
1905.1	(10^-)	(8^-)	874.8	30(7)	
1941.5	11^+	10^+	568.8	43(6)	0.54(18)
		9^+	963.6	5(1)	
2455.6	(11^-)	(9^-)	992.4	15(5)	
2586.2	(12^+)	10^+	1213.5	41(6)	0.81(31)
3016.6	(12^-)	(10^-)	1111	25(5)	
3150	(13^+)	(12^+)	563.6	19(3)	0.72(34)
		11^+	1208.3	18(3)	0.95(31)
3620.0	(13^-)	(11^-)	1164	18(3)	
4050	(14^+)	(12^+)	1464	16(3)	
4297	(14^-)	(12^-)	1280	14(2)	
4543	(15^+)	(13^+)	1393	8(1)	
4922	(15^-)	(13^-)	1302	16(3)	
5605	(16^+)	(14^+)	1555	8(1)	
6088	(17^+)	(15^+)	1545	7(1)	

[a]Normalized to the 100 keV transition.

at 194 and 197 keV excitation [19]. The possibility that the 196 keV line could be a doublet cannot be ruled out in the present experiment. A further complication in the analysis of our data is a 195 keV transition in ^{74}Br, which is also produced in this reaction.

IV. DISCUSSION

A. Cranking-model analysis

A cranking-model analysis [20] was applied to the two rotational bands in ^{78}Br. The kinematic moments of inertia ($\mathcal{J}^{(1)}$) for the positive-parity band in ^{78}Br are shown in Fig. 7. Also plotted, for comparison, are the $\mathcal{J}^{(1)}$'s for the positive-parity yrast bands in ^{74,76}Br, ^{80}Rb, ^{82}Y, and ^{84}Nb. It can be seen that the $\mathcal{J}^{(1)}$ values decrease substantially from the lowest frequencies to $\hbar\omega \approx 0.4$ MeV and remain fairly constant at values ranging from $18\hbar^2$ MeV^{-1} to $23\hbar^2$ MeV^{-1} at higher frequencies, close to the rigid-body values for these nuclei. The decrease of $\mathcal{J}^{(1)}$ at low spin in these nuclei arises from the single-particle motion of the unpaired nucleons; alignment of these particles with the rotational axis is energetically ''inexpensive,'' and so appears as a large moment of inertia in the cranking interpretation.

At a frequency of $\hbar\omega \approx 0.75$ MeV there is a slight increase in $\mathcal{J}^{(1)}$ for the $\alpha = 0$ sequence in ^{78}Br. This can be seen more clearly in plots of the dynamic moments of inertia, $\mathcal{J}^{(2)}$, shown in Fig. 8. The proton upbend seen at $\hbar\omega \approx 0.5$ MeV in the ground-state bands of the neighboring even-even nucleus ^{76}Se [21] is blocked in this nucleus. The neutron alignment reported in ^{77}Br [4] is also blocked in ^{78}Br. A recent investigation of ^{79}Kr [22] found a second crossing in the yrast band at $\hbar\omega \approx 0.75$ MeV and tentatively attributed it to a neutron alignment, based on systematics. It is likely that the upbend seen here in ^{78}Br has the same origin. The data from ^{82}Y, which are available for higher spins, show a crossing in the $\alpha = 0$ sequence at $\hbar\omega \approx 0.6$ MeV. This has also been attributed to a neutron crossing [7].

Experimental Routhians for ^{78}Br as a function of the rotational frequency are shown in Fig. 9, where they are compared with Routhians of neighboring isotopes and isotones. For consistency, the reference parameters defined by Chishti *et al.* [23] were used. The signature inversion common in positive-parity bands in this region can be seen in this figure. The experimental Routhians for the signature partners in each nucleus show a small amount of splitting at lower frequencies and cross at frequencies of about 0.35, 0.45, and

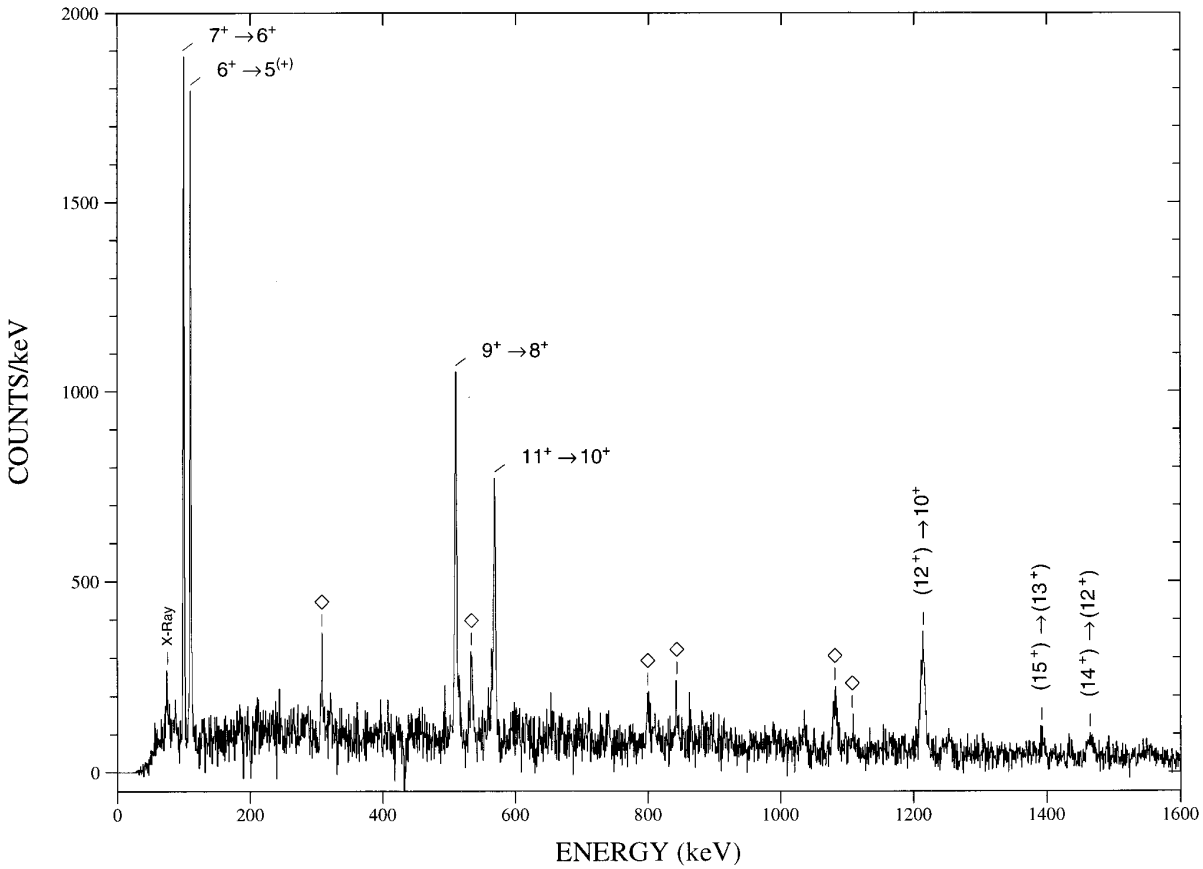

FIG. 4. The spectrum of γ rays produced by gating on the 394 and 905 keV lines. Diamonds indicate transitions in ^{77}Br.

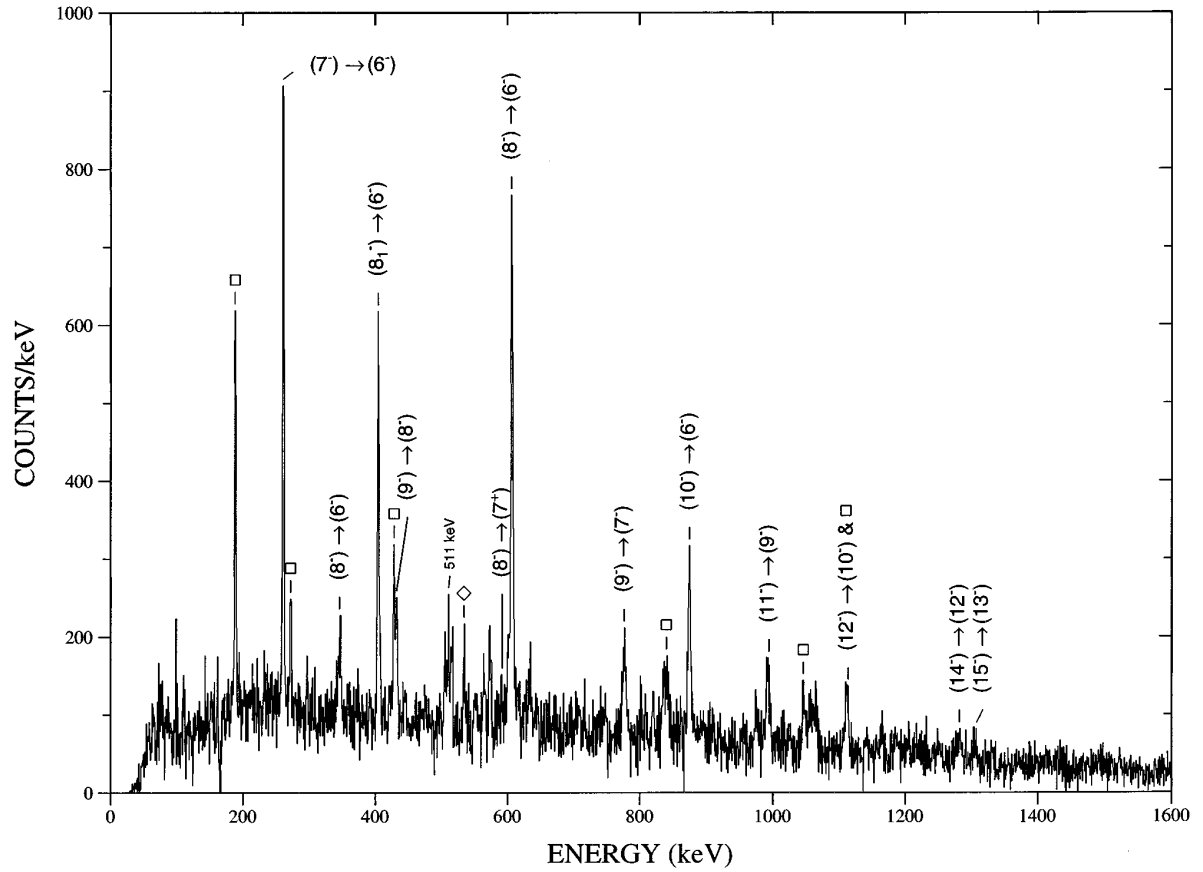

FIG. 5. The spectrum of γ rays produced by gating on the 196 keV line. Squares indicate transitions in ^{74}Br. Diamonds indicate transitions in ^{77}Br.

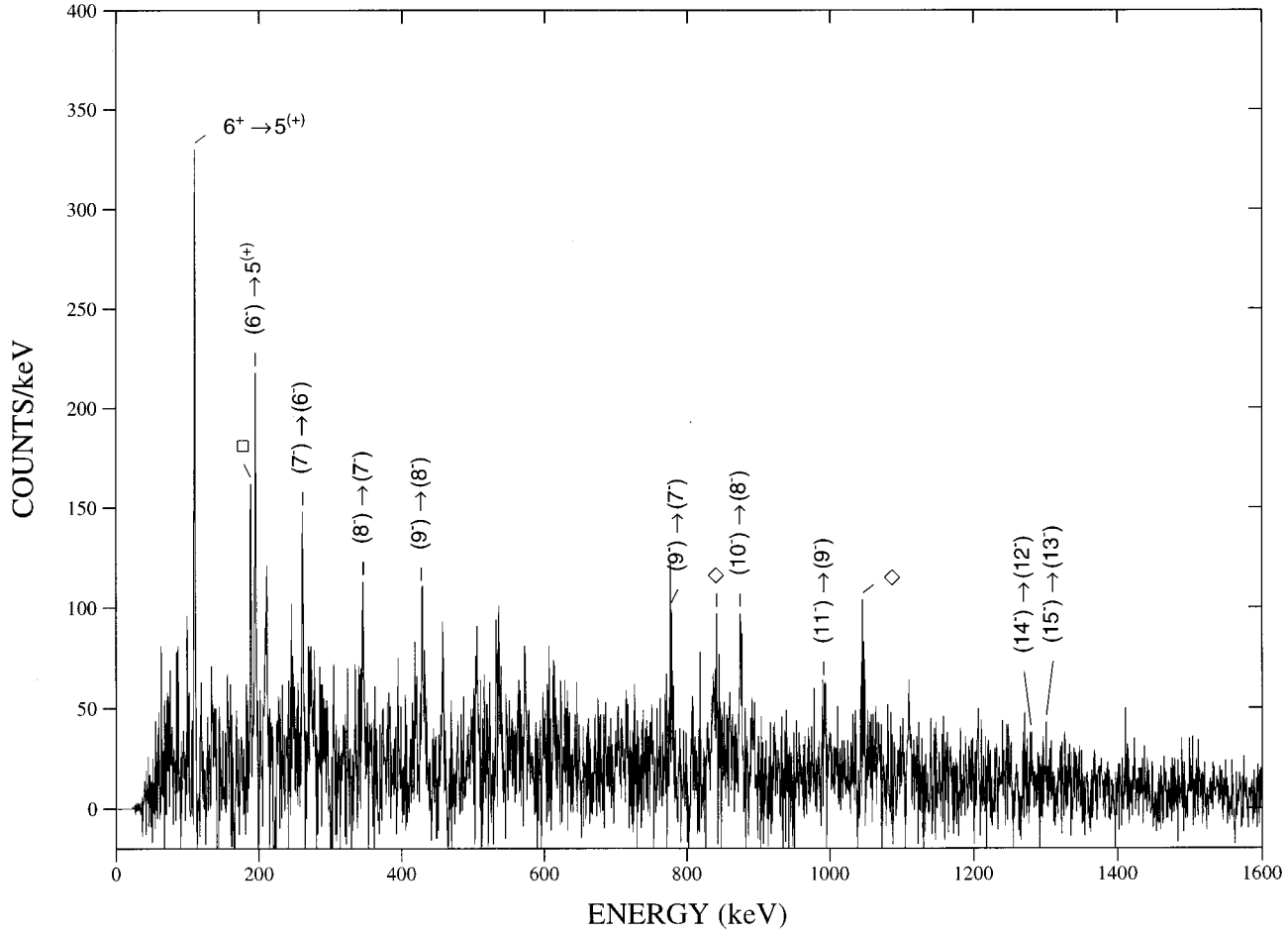

FIG. 6. The spectrum of γ rays produced by gating on the 345 keV line. Squares indicate transitions in ^{74}Br. Diamonds indicate transitions in ^{77}Br.

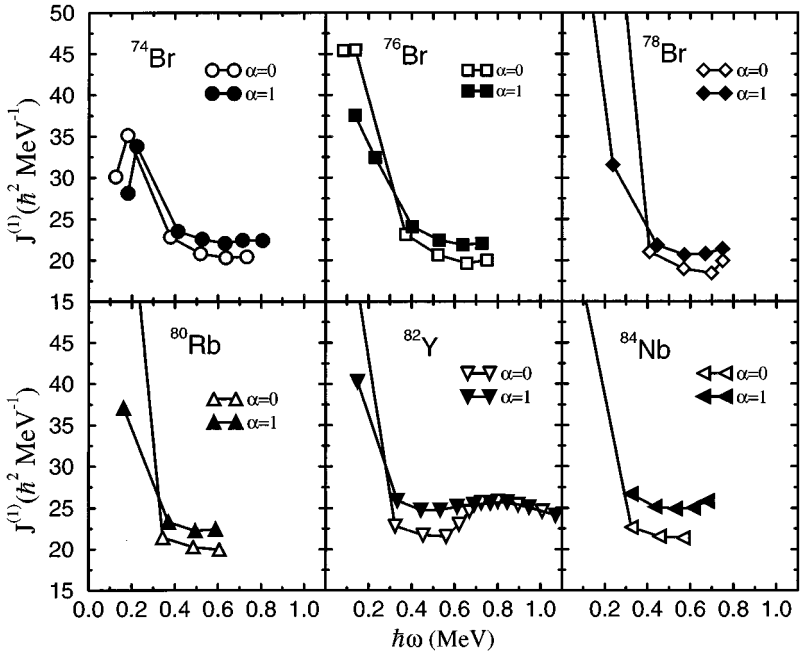

FIG. 7. The kinematic moments of inertia for the yrast bands of ^{74,76,78}Br, ^{80}Rb, ^{82}Y, and ^{84}Nb as a function of rotational frequency. The points for the lowest frequencies are off scale due to the expanded ordinate.

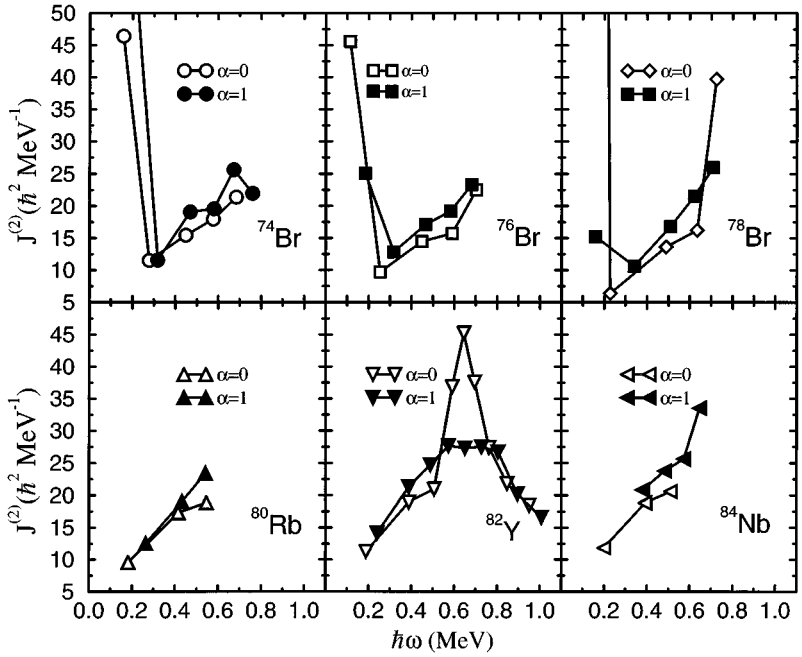

FIG. 8. The dynamic moments of inertia for the yrast bands of the same bands as shown in Fig. 7.

0.55 MeV for ^{74,76,78}Br, respectively. At higher frequencies, the splitting increases. A similar pattern is observed for the isotones ^{80}Rb and ^{82}Y with the inversion occurring at 0.45 MeV for ^{80}Rb and 0.35 MeV for ^{82}Y.

The signature splitting and inversion are best visualized by plotting the experimental quantity $(E_I - E_{I-1})/2I$ as a function of spin, as shown in Fig. 10. The signature inversions can be seen as a reversal in the phase of the staggering. The spins at which the inversion occurs are $I = 9\hbar$, $11\hbar$, and $11\hbar$ for ^{74,76,78}Br and $I = 11\hbar$, $9\hbar$, and $9\hbar$ for ^{80}Rb, ^{82}Y, and ^{84}Nb, respectively. After this inversion the splitting becomes more pronounced and reaches a limit ranging from $\approx$ 18 to 35 keV, with the largest splitting occurring in the heaviest isotone. The splitting at high spin is approximately 25 keV for all of the Br isotopes; clearly, the magnitude of splitting at high spin changes more drastically with Z than with N. Similar plots for negative-parity bands in these nuclei show no evidence of inversion. Previous discussions of signature inversion in this mass region [1,6,13], based on particle-plus-rotor approaches, have argued that the inversion of signature splitting should occur after the highest value available from the intrinsic motion of two $g_{9/2}$ particles in an odd-odd nucleus has been reached. This value is $9\hbar$ for the $\pi g_{9/2} \otimes \nu g_{9/2}$ configuration, above which the rotational band can be generated by collective motion. As mentioned above, the change from single-particle to collective motion is noticeable in the kinematic moment of inertia at frequencies around 0.4 MeV, where the values level off after a sharp drop. Figure 10 shows, however, that the inversion does not take place at a spin of $I = 9\hbar$ for all cases.

Kinematic moments of inertia for the negative-parity rotational sequences in ^{78}Br are shown in Fig. 11, with one of

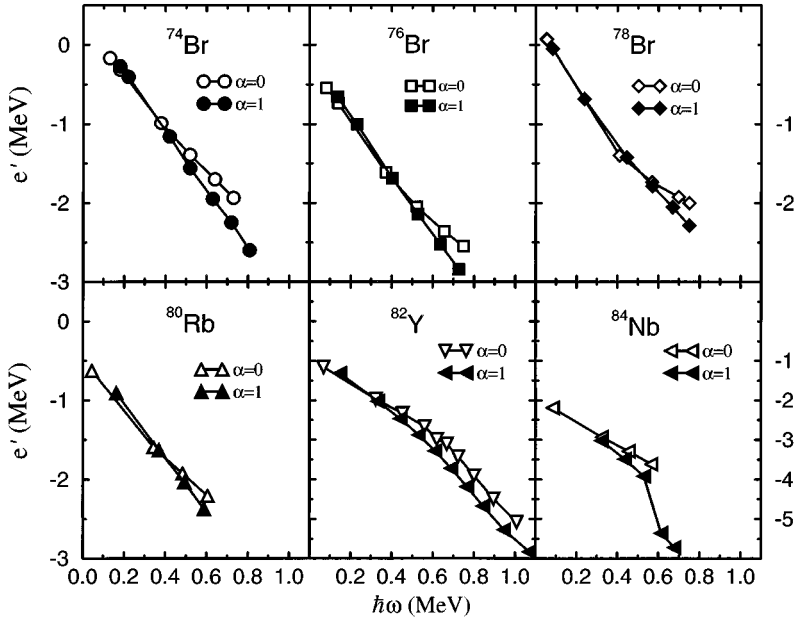

FIG. 9. The experimental Routhians for the yrast bands of the same bands as shown in Fig. 7.

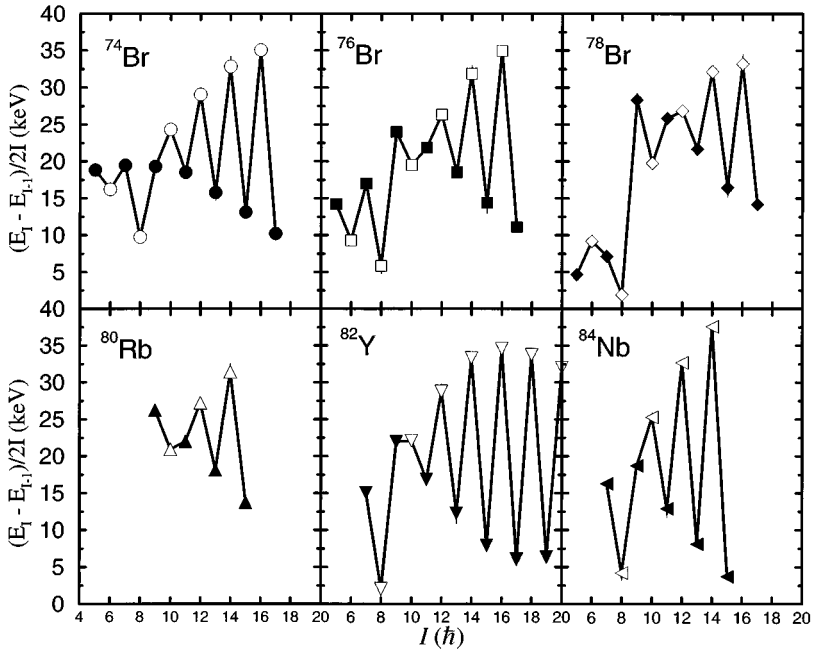

FIG. 10. Plots of the quantity $(E_I - E_{I-1})/2I$ as a function of spin for the yrast bands in ^{74,76,78}Br, ^{80}Rb, ^{82}Y, and ^{84}Nb.

the positive-parity sequences included for comparison. Throughout the range observed, the values for the negative-parity sequences are nearly constant and close to the rigid-body value. The nature of the negative-parity states in these sequences is not well understood at this point. In ^{77}Br, a negative-parity, $K=\frac{3}{2}$ band is believed to be built on a $\pi[301]\frac{3}{2}^-$ configuration [4], while for ^{76}Br it has been suggested that negative-parity rotational sequences are built on neutron $g_{9/2}$ excitations coupled to protons occupying negative-parity orbitals [9]. Within the context of the current work, it is not possible to make a definite assignment for this band in ^{78}Br.

B. Cranked mean-field calculations

Cranked-shell-model calculations were performed in order to help interpret the experimental results. A deformed Woods-Saxon potential was used, and residual interactions were modeled using a monopole pairing term. Self-consistency in the pairing was required for all rotational frequencies. In order to calculate total Routhians, the Strutinsky shell correction was applied. For a more detailed description of the calculations, see Refs. [24,25] and references quoted therein. The only adjustable parameters in the calculation are the pairing strengths G for protons and neutrons; the values used for ^{78}Br were $23.0/A$ MeV for protons and $21.2/A$ MeV for neutrons.

Total Routhian surfaces (TRS's) for ^{78}Br are shown in Fig. 12. Calculations were run on a 15×17 point mesh in the (β_2,γ) plane, and values of β_4 were chosen to minimize the total Routhian for each point on the grid. The surface at a rotational frequency of $\hbar\omega=0.2$ MeV is shown in the left side of the figure. As the rotational frequency increases some of the minima disappear and the nucleus becomes more γ soft at $\hbar\omega=0.6$ MeV. Shape coexistence, seen in the form of several minima, is evident in the surfaces. Many of the observed minima lie close in energy, making the assignment of a particular shape to the yrast band difficult. It was found, however, that a reasonable match between calculated and experimental moments of inertia occurred only at the minimum with deformation parameters $(\beta_2,\gamma) = (0.32, 21.3°)$. A plot of the experimental and theoretical values for $\mathfrak{I}^{(1)}$ is shown in Fig. 13. The corresponding calculated quasiparticle

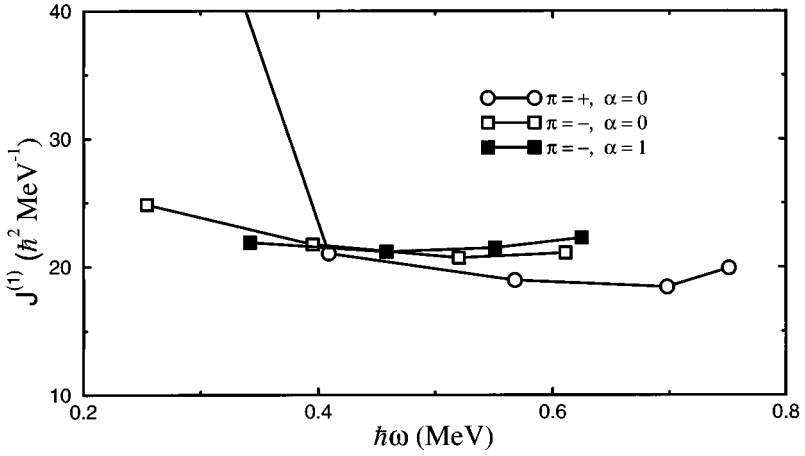

FIG. 11. The kinematic moments of inertia for the negative-parity sequences in ^{78}Br, compared with the positive-parity, even-spin sequence.

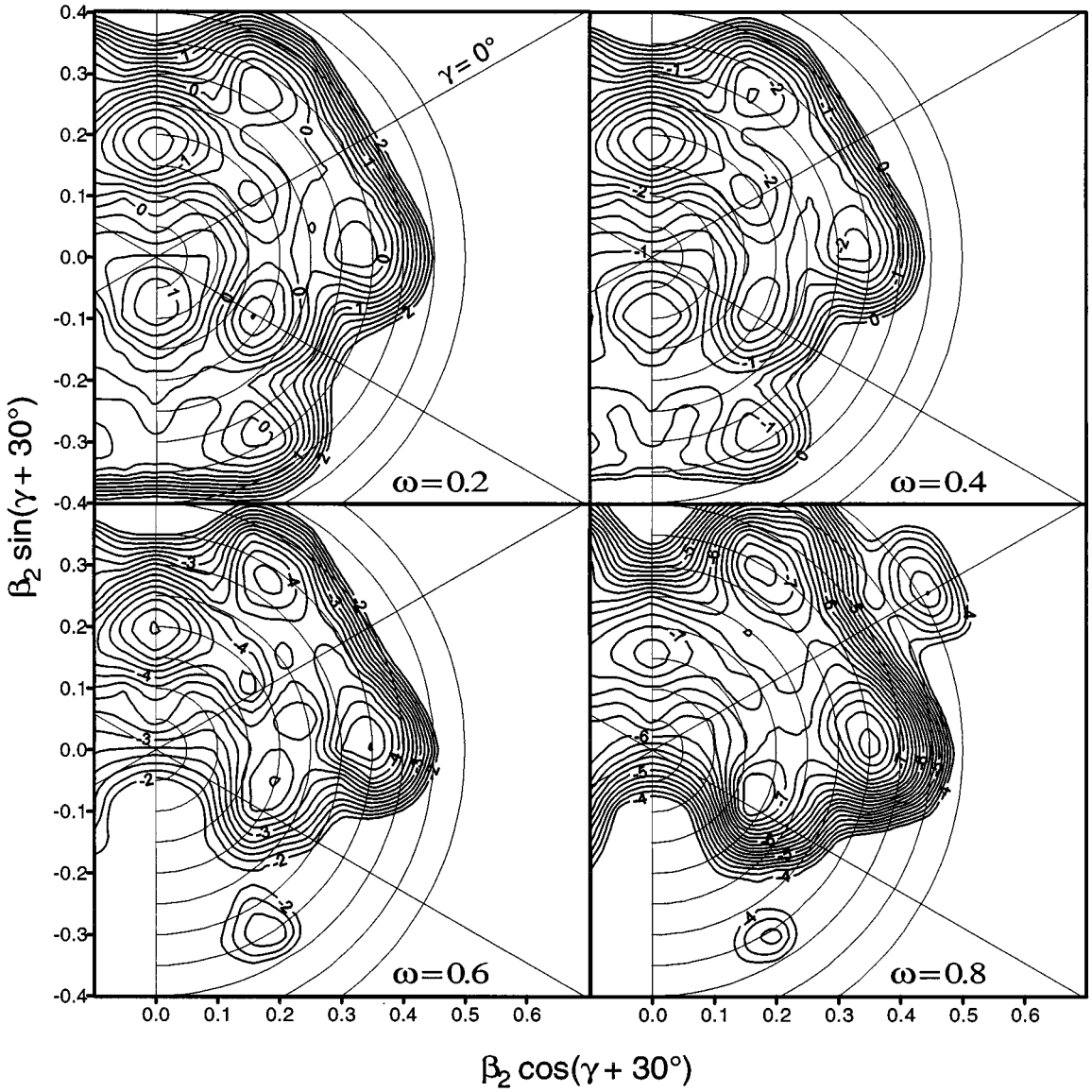

FIG. 12. Total Routhian surfaces for ^{78}Br. The angular frequencies used are indicated in the lower right portion of each panel, in units of MeV/$\hbar$. Routhians were calculated using the ''aB''$(\pi,\alpha)=(+,0)$ configuration. The deformation parameter β_4 was chosen to minimize the Routhian at each point on the grid. Contour interval is 0.2 MeV.

Routhians are shown in Fig. 14. The labels shown in the figure follow the convention of labeling the lowest unique-parity Routhians as a (or A) and b (or B) for the $\alpha=+1/2$ and $\alpha=-1/2$ signatures, respectively.

Calculated and experimental signature splitting is shown in Fig. 15 for the yrast band of ^{78}Br as well as for the isotopes ^{74,76}Br and the isotone ^{82}Y. The difference between the Routhians for the $\alpha=1$ signature partner and the $\alpha=0$ signature partner is plotted as a function of angular frequency. Symbols indicate the experimentally derived values, and the four lines in each panel show the calculated quantities based on the four possible combinations of configuration. Lower case letters indicate the proton configuration, upper case the neutron configuration. Calculations were performed for ^{74,76}Br and ^{82}Y in the same way as was done for ^{78}Br. That is, TRS's were calculated with self-consistent pairing and the deformations used in the figure were chosen on the basis of minimum energy in the TRS's and fits to the kinematic moments of inertia. For each of the bromine isotopes the deformation was found to be triaxial with $\gamma>0°$, while for ^{82}Y the deformation has $\gamma<0°$. For all of the nuclei shown, the best theoretical match is given by the quantity $aA-aB$, although for ^{82}Y the difference between this quantity and $aA-bA$ is slight. For the three bromine isotopes, the match between the theoretical and experimental values for signature splitting is in good agreement both in magnitude and in the frequency at which the inversion occurs. The agreement for ^{82}Y is also good, though the inversion is not reproduced by the calculations.

These results are in agreement with work by Bengtsson *et al.* [12] in which the relationship between signature inversion and triaxiality is examined. In that work, there are two conditions given that need to be met in order for signature inversion to occur. First, the nucleus has to be triaxial with $\gamma>0°$ so that there is an orbital for which the unfavored signature is down sloping at zero frequency. Second, the

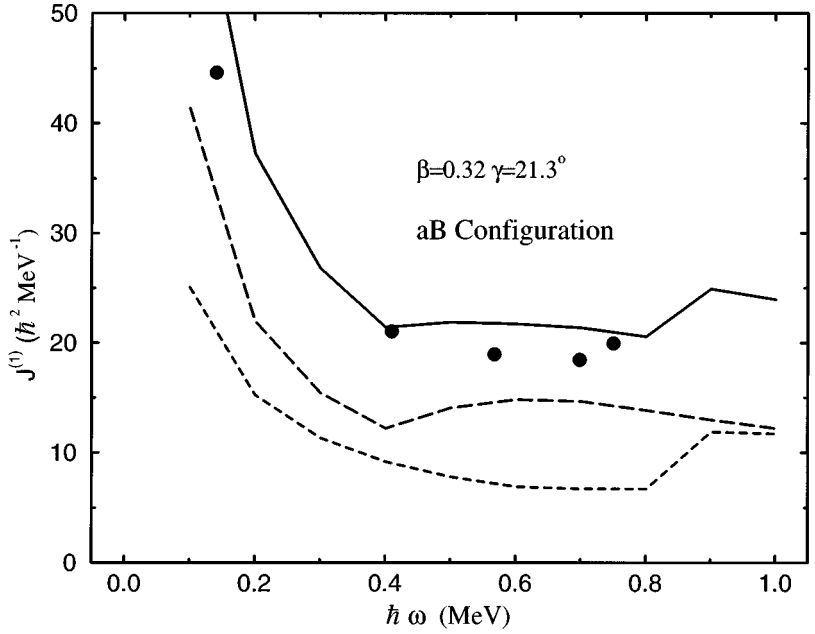

FIG. 13. Calculated and experimental kinematic moment of inertia for the positive-parity yrast band in ^{78}Br. The long-dashed and short-dashed lines correspond to the proton and neutron contributions, respectively.

$K=\frac{3}{2}$ orbital must lie closer to the Fermi surface than the $K=\frac{1}{2}$ orbital. When this latter requirement is satisfied, mixing of the $K=\frac{1}{2}$ orbital with the $K=\frac{3}{2}$ and $K=\frac{5}{2}$ orbitals results in signature inversion. In the bromine isotopes, the key orbitals involved in the signature inversion are the neutron $g_{9/2}$ orbitals with asymptotic quantum numbers $[440]\frac{1}{2}$, $[431]\frac{3}{2}$, and $[422]\frac{5}{2}$.

It is also noted in Ref. [12] that signature inversion might be expected to occur for oblate shape ($\gamma\approx 60°$) for nuclei with N or Z equal to 41 or 43. While our calculations for ^{78}Br show an oblate minimum in the TRS, we were not able reproduce the signature inversion at this deformation.

It should be noted that there are arguments [26] suggesting that an observed signature inversion in odd-odd nuclei may not be sufficient evidence for a triaxial shape when a high-j configuration is taken and the inversion is observed at relatively low spins. It is also the case, as noted above, that particle-rotor calculations can in some cases reproduce signature inversion for axially symmetric shapes when a proton-

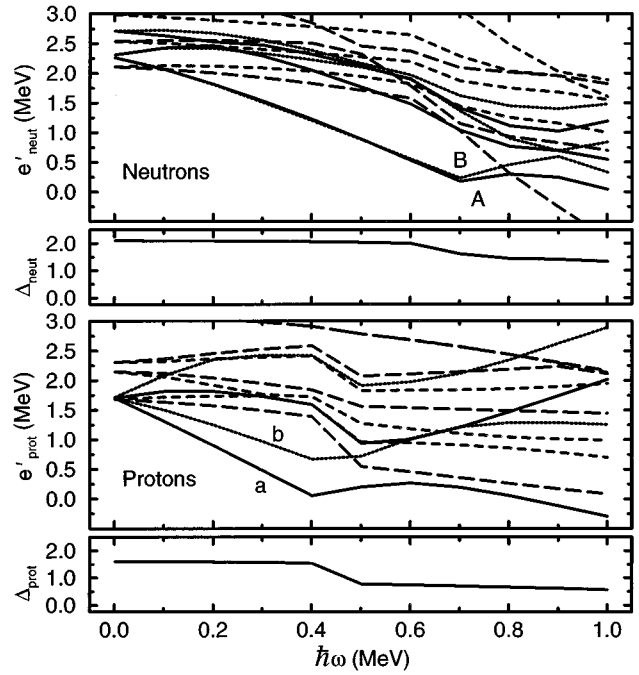

FIG. 14. Calculated quasiparticle Routhians for the deformation $(\beta_2,\gamma)=(0.32, 21.3°)$. Solid lines correspond to Routhians with $(\pi,\alpha)=(+,+1/2)$, dotted lines to $(+,-1/2)$, long-dashed lines to $(-,+1/2)$, and short-dashed lines to $(-,-1/2)$. Also shown are calculated values of the pair-gap parameter Δ for protons and neutrons.

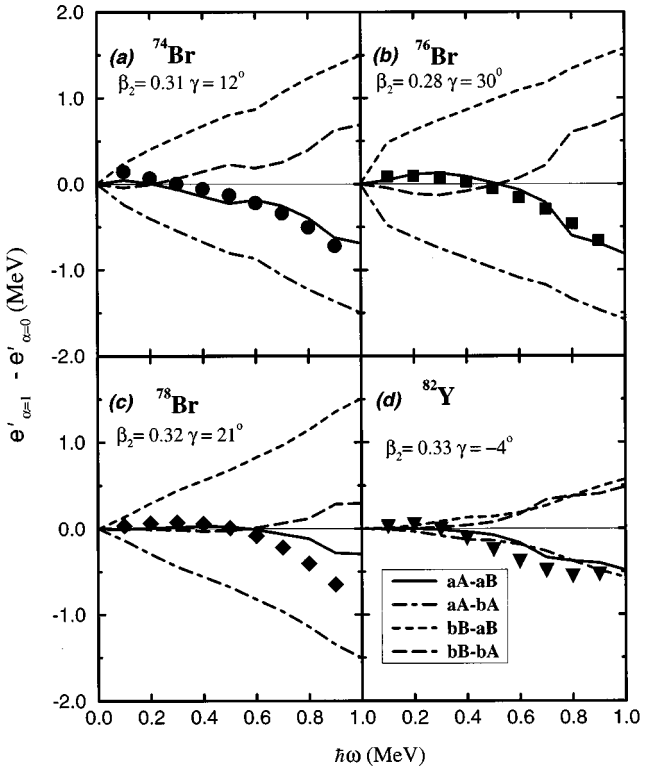

FIG. 15. Calculated and experimental signature splitting in ^{78}Br and neighboring odd-odd nuclei.

neutron interaction is included. In the case of the present work, however, the excellent agreement between experiment and theory for both moment of inertia and signature inversion indicates a probable triaxial shape for ^{78}Br.

V. CONCLUSIONS

Several new high-spin states were found in the odd-odd nucleus ^{78}Br, including several states in a previously unobserved rotational band. As in nearby odd-odd nuclei, signature inversion is seen in the positive-parity yrast band. Cranked-shell-model calculations reproduce the magnitude of the signature splitting and the frequency at which it occurs surprisingly well. Signature splitting and inversion are both sensitive to quasiparticle configuration. This sensitivity allows the assignment of the quasiparticle configuration of the positive-parity yrast bands.

ACKNOWLEDGMENTS

This work was funded by the National Science Foundation. One of the authors (E.L.) received support from Conselho Nacional de Desenvolvimento e Pesquisa (CNPq), Brasil. Professor J. Dudek of Strasbourg supplied the cranked-shell-model codes used in this work.

[1] J.W. Holcomb, T.D. Johnson, P.C. Womble, P.D. Cottle, S.L. Tabor, F.E. Durham, and S.G. Buccino, Phys. Rev. C **43**, 470 (1991)
[2] D.F. Winchell, Ph.D. thesis, University of Pittsburgh, 1990.
[3] S.G. Buccino, F.E. Durham, J.W. Holcomb, T.D. Johnson, P.D. Cottle, and S.L. Tabor, Phys. Rev. C **41**, 2056 (1990).
[4] G.N. Sylvan, J.E. Purcell, J. Döring, J.W. Holcomb, G.D. Johns, T.D. Johnson, M.A. Riley, P.C. Womble, V.A. Wood, and S.L. Tabor, Phys. Rev. C **48**, 2252 (1993).
[5] R. Schwengner, J. Döring, L. Funke, G. Winter, A. Johnson, and W. Nazarewicz, Nucl. Phys. **A509**, 550 (1990).
[6] P.C. Womble, J. Döring, T. Glasmacher, J.W. Holcomb, G.D. Johns, T.D. Johnson, T.J. Petters, M.A. Riley, V.A. Wood, S.L. Tabor, and P. Semmes, Phys. Rev. C **47**, 2546 (1993).
[7] S.D. Paul, H.C. Jain, S. Chattopadhyay, M.L. Jhingan, and J.A. Sheikh, Phys. Rev. C **51**, 2959 (1995).
[8] J. Döring, J.W. Holcomb, T.D. Johnson, M.A. Riley, S.L. Tabor, P.C. Womble, and G. Winter, Phys. Rev. C **47**, 2560 (1993).
[9] D.F. Winchell, J.X. Saladin, M.S. Kaplan, and H. Takai, Phys. Rev. C **41**, 1264 (1990).
[10] J. Döring, G. Winter, L. Funke, B. Cederwall, F. Lidén, A. Johnson, A. Atac, J. Nyberg, G. Sletten, and M. Sugawara, Phys. Rev. C **46**, R2127 (1992).
[11] C.J. Gross, K.P. Lieb, D. Rudolph, M.A. Bentley, W. Gelletly, H.G. Price, J. Simpson, D.J. Blumenthal, P.J. Ennis, C.J. Lister, Ch. Winter, J.L. Durell, B.J. Varley, Ö. Skeppstedt, and S. Rastikerdar, Nucl. Phys. **A535**, 203 (1991).
[12] R. Bengtsson, H. Frisk, F.R. May, and J.A. Pinston, Nucl. Phys. **A415**, 189 (1984).
[13] A.J. Kreiner and M.A.J. Mariscotti, Phys. Rev. Lett. **43**, 1150 (1979).
[14] P.B. Semmes and I. Ragnarsson, in *Proceedings of the International Conference on High Spin Physics and Gamma-Soft Nuclei*, edited by J.X. Saladin, R.A. Sorenson, and C.M. Vincent (World Scientific, Singapore, 1991).
[15] J. Döring, F. Dubbers, L. Funke, P. Kemnitz, E. Will, and G. Winter, Rossendorf Annual Report 1980, No. ZFK-443, 1981.
[16] M. Behar, D. Abriola, A. Filevich, G. García Bermúdez, A.J. Kreiner, and M.A.J. Mariscotti, Nucl. Phys. **A376**, 131 (1982).
[17] J.X. Saladin, IEEE Trans. Nucl. Sci. **NS-30**, 420 (1983).
[18] S.L. Tabor, M.A. Riley, J. Döring, P.D. Cottle, R. Books, T. Glasmacher, J.W. Holcomb, J. Hutchins, G.D. Johns, T.D. Johnson, T. Petters, O. Tekyi-Mensah, P.C. Womble, L. Wright, and J.X. Saladin, Nucl. Instrum. Methods Phys. Res. B **79**, 821 (1993).
[19] C.M. Lederer and V.S. Shirley, *Table of Isotopes* (Wiley, New York, 1978).
[20] R. Bengtsson, S. Frauendorf, and F.-R. May, At. Data Nucl. Data Tables **35**, 15 (1986).
[21] J.C. Wells, R.L. Robinson, H.J. Kim, R.O. Sayer, R.B. Piercey, A.V. Ramayya, J.H. Hamilton, and C.F. Maguire, Phys. Rev. C **22**, 1126 (1980).
[22] G.D. Johns, J. Döring, J.W. Holcomb, T.D. Johnson, M.A. Riley, G.N. Sylvan, P.C. Womble, V.A. Wood, and S.L. Tabor, Phys. Rev. C **50**, 2786 (1994).
[23] A.A. Chishti, W. Gelletly, C.J. Lister, J.H. McNeill, B.J. Varley, D.J.G. Love, and Ö Skeppstedt, Nucl. Phys. **A501**, 568 (1989).
[24] W. Nazarewicz, J. Dudek, R. Bengtsson, T. Bengtsson, and I. Ragnarsson, Nucl. Phys. **A435**, 397 (1985).
[25] D.F. Winchell, M.S. Kaplan, J.X. Saladin, H. Takai, J.J. Kolata, and J. Dudek, Phys. Rev. C **40**, 2672 (1989).
[26] I. Hamamoto, Phys. Lett. B **235**, 221 (1990).